APPLIED AND ENVIRONMENTAL MICROBIOLOGY, Nov. 2005, p. 6934–6946 Vol. 71, No. 11
0099-2240/05/$08.00+0 doi:10.1128/AEM.71.11.6934–6946.2005

Identifying Components of the NF-κB Pathway in the Beneficial *Euprymna scolopes-Vibrio fischeri* Light Organ Symbiosis†

Michael S. Goodson,[1] Mila Kojadinovic,[1]‡ Joshua V. Troll,[1] Todd E. Scheetz,[2] Thomas L. Casavant,[2,3] M. Bento Soares,[4] and Margaret J. McFall-Ngai[1]*

Department of Medical Microbiology and Immunology, University of Wisconsin, Madison, Wisconsin 53706,[1] and Center for Bioinformatics and Computational Biology and Departments of Biomedical Engineering and Opthalmology,[2] Department of Electrical and Computer Engineering,[3] and Department of Pediatrics,[4] University of Iowa, Iowa City, Iowa 52242

Received 1 April 2005/Accepted 1 July 2005

The Toll/NF-κB pathway is a common, evolutionarily conserved innate immune pathway that modulates the responses of animal cells to microbe-associated molecular patterns (MAMPs). Because MAMPs have been implicated as critical elements in the signaling of symbiont-induced development, an expressed sequence tag library from the juvenile light organ of *Euprymna scolopes* was used to identify members of the Toll/NF-κB pathway. Full-length transcripts were identified by using 5′ and 3′ RACE PCR. Seven transcripts critical for MAMP-induced triggering of the Toll/NF-κB phosphorylation cascade have been identified, including receptors, signal transducers, and a transcription factor. Further investigations should elucidate the role of the Toll/NF-κB pathway in the initiation of the beneficial symbiosis between *E. scolopes* and *Vibrio fischeri*.

Microbe-associated molecular patterns (MAMPs), such as lipopolysaccharide (LPS), peptidoglycan (PGN), and CpG DNA, are active in initiating innate immune responses in both animals and plants (32, 39, 70). In such responses, the binding of MAMPs to receptors often triggers signal transduction pathways, including the Toll/NF-κB pathway, that have striking similarities among these phylogenetically diverse organisms (Fig. 1) (5, 30, 51). The highly conserved Toll/NF-κB signaling pathway has been studied extensively for its role in microbial pathogenesis in two of the three major branches of the animal kingdom, the vertebrates (Deuterostomia) and the insects (Ecdysozoa) (1, 21, 64). The NF-κB family proteins exist in unstimulated cells of these animals as homo- or heterodimers that are sequestered in the cytoplasm by a member of the Inhibitor of NF-κB (IκB) proteins. Through interaction with a receptor, MAMPs elicit an intracellular phosphorylation cascade. This phosphorylation cascade converges on, and activates, a complex of serine kinases termed IκB kinases (IKKs) (35). The IKK complex phosphorylates serine residues of IκB, leading to its ubiquitination and degradation by the proteosome (25). Degradation of IκB allows the NF-κB dimer to translocate into the nucleus and activate transcription of target genes possessing the κB promoter site. Although evidence is available for the presence of the NF-κB pathway in a mollusk, the Pacific oyster (20, 28, 48), the signaling pathways activating the immune responses in mollusks and other Lophotrochozoa, the members of which form the third branch of the animal kingdom (2, 29, 59), are largely unknown (Fig. 1).

Euprymna scolopes is a cephalopod mollusk that has been used as a model for the study of the establishment and maintenance of beneficial animal-bacterial symbioses (53). This Hawaiian squid species harbors the marine luminous bacterium *Vibrio fischeri* in a complex light organ in the center of its body cavity. Several studies of this association have implicated MAMPs as the molecules that mediate the early symbiont-induced development of the juvenile light organ. Specifically, the PGN fragments released by environmental bacteria induce the newly hatched, uncolonized juvenile *E. scolopes* to secrete mucus from a complex field of epithelial cells on the surface of the organ (52, 54). After *V. fischeri* gathers in this mucus outside the light organ, it enters pores and travels down ducts to epithelium-lined crypt spaces, where it induces mucus shedding by the crypt epithelial cells (52). Once inside the crypts, the symbiont also triggers the cessation of mucus shedding by the superficial field of ciliated epithelial cells (52) and loss of this field over the first 4 days of the symbiosis by apoptosis (24) and regression (18, 49). Experimental analysis of these developmental events has demonstrated that the synergistic interactions of derivatives of symbiont LPS and PGN are capable of inducing the exact pattern of *V. fischeri*-induced light organ morphogenesis (23, 39).

Both biochemical and cellular evidence have suggested that, during the complex program of early host light organ development, *V. fischeri* MAMPs signal and activate host cells through pathways either analogous or homologous to the Toll/NF-κB signaling pathway. For example, mucus secretion, as a response to interactions with bacteria, is controlled by the Toll/NF-κB pathway in other systems (34, 40, 63). In addition, the activities of halide peroxidase (58, 65, 71) and nitric oxide synthase (16) have been implicated in the dynamics of the squid-vibrio system, and the transcription of the genes that encode these proteins is either directly or indirectly activated by NF-κB in other hosts (4, 60). At the cellular level, the

* Corresponding author. Mailing address: Department of Medical Microbiology and Immunology, University of Wisconsin, 1300 University Ave., Madison, WI 53706. Phone: (608) 262-2393. Fax: (608) 262-8418. E-mail: mjmcfallngai@wisc.edu.

† Supplemental material for this article may be found at http://aem.asm.org/.

‡ Present address: CEA Cadarache DEVM/LBC–Bat 156, 13108 Saint Paul-Lez-Durance Cedex, France.

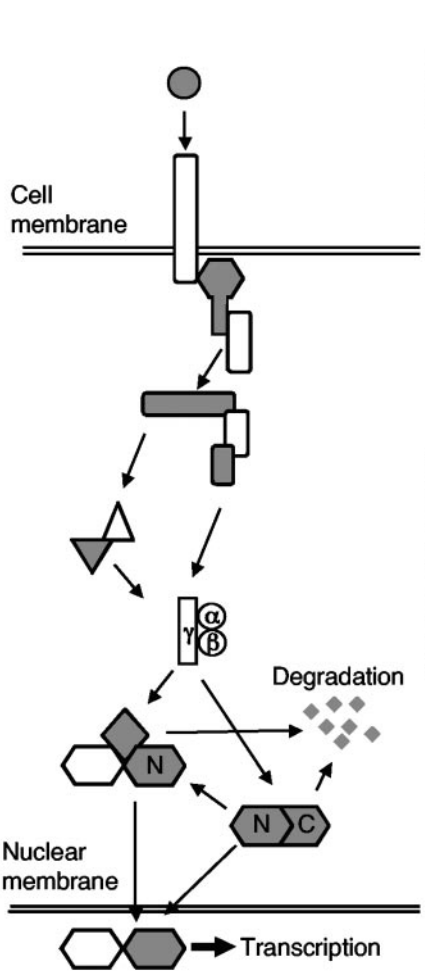

	Deuterostomia	Ecdysozoa	Lophotrochozoa	Plantae
MAMP	LPS, PGN, ssRNA, CpG DNA, flagellin	LPS, PGN, fungal proteins	ND*	LPS, flagellin
Receptor	TLRs, PGRPs, NODs	Toll, PGRPs	AiPGRP [EsToll] [EsPGRP1-4]	R gene products: Xa21, FLS2
Signal transduction	MyD88	Tube, Imd		
	IRAK	Pelle	[EsIRAK4]	pto, pti, fen, FLS2 kinase
	TRAF	dTRAF	[EsTRAF6]	
	TAK	dTAK		
	TAB	TAB-like		
	ECSIT	dECSIT		
	MEKK	dMEKK		AtMEKK
	IKK complex: IKKα, IKKβ, IKKγ/NEMO	DmIKK complex: kenny, ird5	oIKKα [EsIKKγ]	
	IκB	Cactus	[EsIκB]	IκB-like
	NF-κB p65 NF-κB p50	Dorsal, Dif	Cg-REL [EsREL]	WRKY22/29
	NF-κB p105	Relish		

FIG. 1. The signaling pathways activating the innate immune responses of plants and animals are similar. NF-κB p105 and Relish have a REL homology domain located at their N terminus (N) and an IκB-like domain at their C terminus. The C terminus domain can be proteolytically cleaved and degraded. Brackets enclose pathway members identified in the present study. The molecules listed in the figure represent full-length sequences. Ai, *Argopecten irradians*; At, *Arabidopsis thaliana*; C, C terminus; Cg, *Crassostrea gigas*; CpG DNA, unmethylated CG dinucleotides prevalent in bacterial DNA; d, drosophila; ECSIT, evolutionarily conserved signaling intermediate in Toll pathways; Es, *Euprymna scolopes*; IκB, inhibitor of NF-κB; IKK, IκB kinase; Imd, immune deficiency; IRAK, interleukin-1-receptor-associated kinase; ird, immune response deficient; LPS, lipopolysaccharide; MEKK, mitogen-activated protein kinase/extracellular signal-regulated kinase kinase kinase; MyD88, myeloid differentiation primary response gene 88; N, N terminus; ND*, not determined that MAMPs activate this pathway in this superphylum; NEMO, NF-κB essential modulator; NF-κB, nuclear factor κB; NIK, NF-κB inducing kinase; NOD, nucleotide-binding oligomerization domain protein; o, oyster; PGN, peptidoglycan; PGRP, PGN recognition proteins; R gene, plant resistance genes; REL, proteins containing regions of homology to the *rel* oncogene, the definition of the NF-κB family of genes; ssRNA, single-stranded RNA; TAB, TAK-binding protein; TAK, transforming growth factor β-activated kinase 1; TLR, Toll-like receptor; Tollip, Toll interacting protein; TRAF, tumor necrosis factor receptor-associated factor.

recruitment of macrophage-like hemocytes into the light organ (39) and apoptosis of the cells of the superficial ciliated epithelium (24) are types of cellular behaviors modulated by activity of the NF-κB pathway in many host-pathogen interactions (13, 33, 36, 41, 55).

In the present study, we used juvenile light organ expressed sequence tag (EST) libraries to search for transcripts encoding proteins of the Toll/NF-κB pathway and rapid amplification of cDNA ends (RACE) PCR to obtain full-length sequences. Our data provide evidence that the pathway is present in *E. scolopes*, a finding that paves the way for the study of its regulation in beneficial animal-bacterial interactions using the squid-vibrio model.

MATERIALS AND METHODS

General procedures. Adult *E. scolopes* organisms were collected from shallow sand flats of Oahu, Hawaii, and breeding colonies were maintained as described previously (18, 23). Upon hatching, the juvenile *E. scolopes* organisms were rinsed and placed individually in 5 ml of either offshore seawater, which does not contain sufficient quantities of *V. fischeri* to result in colonization, or offshore seawater containing 5×10^3 cells ml^{-1} of wild-type *V. fischeri* strain ES114 (10). Colonization of the light organ was monitored by using a photometer (TD-20/20 luminometer; Turner Designs, Sunnydale, CA) to measure bacterial luminescence emitted by each animal. Unless otherwise stated, reagents used were purchased from Sigma-Aldrich (St. Louis, MO).

Molecular analysis. Candidate sequences were identified by analyses of a light organ EST database that had been constructed by using juvenile *E. scolopes* light organs (EST sequences available through The Wellcome Trust Sanger Institute and European Bioinformatics Institute [http://trace.ensembl.org/]). The se-

TABLE 1. *E. scolopes* 3′ ESTs most similar to the molecules of the Toll/NF-κB pathway[e]

Most similar complete sequence in the database			*E. scolopes* 3′ EST		
Protein	Organism[a]	Protein length (aa)	Length (bp)	Region of hit[b] (aa)	E value
Receptors					
Toll-like receptor	*Apis mellifera*	1,248	691	721–947	$2e^{-29}$
PGRP1	*Apis mellifera*	172	785	140–169	$1e^{-2}$
PGRP2	*Xenopus laevis*	182	802	28–180	$3e^{-41}$
PGRP3	No hit[c]		760		
PGRP4	*Argopecten irradians*	189	727	15–188	$6e^{-42}$
LBP	*Crassostrea gigas*	477	785	267–473	$1e^{-8}$
Signaling molecules					
Tollip	*Mus musculus*	274	794	38–273	$1e^{-66}$
IRAK4	*Homo sapiens*	460	748	261–458	$1e^{-36}$
TRAF6	*Rattus norvegicus*	738	716	522–715	$6e^{-35}$
ECSIT	*Mus musculus*	435	678	214–393	$8e^{-22}$
MEKK	*Dictyostelium discoideum*	942	634	287–429	$2e^{-38}$
IKKγ/NEMO	*Homo sapiens*	419	697	235–416	$4e^{-15}$
IκBα	*Gallus gallus*	318	799	118–275	$5e^{-28}$
NF-κB molecules					
RelA/p65	*Crassostrea gigas* Rel1	615	618	313–475	$2e^{-15}$
RELISH/p105	*Mus musculus*	971	736	732–894	$2e^{-11}$
Regulated genes					
MMP[d]	*Homo sapiens*	1,037	658	839–1,034	$9e^{-36}$
Mucin	*Homo sapiens*	2,448	697	2,253–2,390	$2e^{-3}$
Nitric oxide synthase	*Aplysia californica*	1,387	505	1,223–1,348	$6e^{-19}$

[a] *Apis mellifera*, honeybee; *Aplysia californica*, California sea hare; *Argopecten irradians*, bay scallop; *Bombyx mori*, silk moth; *Crassostrea gigas*, Pacific oyster; *Dictyostelium discoideum*, slime mold; *Gallus gallus*, chicken; *Homo sapiens*, human; *Mus musculus*, house mouse; *Rattus norvegicus*, brown rat; *Xenopus laevis*, African clawed frog.

[b] Region of most similar complete sequence in the database that matches the *E. scolopes* EST.

[c] Identified by BLASTn comparison of *E. scolopes* PGRP1, -2, and -4 against the entire squid 3′ EST database.

[d] Matrix metalloproteinase.

[e] Accession numbers of most similar complete sequences in the database from top are as follows: XP_393713, XP_395941, AAH87429, AAR92030, AAN84552, NP_076253, NP_057207, XP_230377, NP_036159, AAC97114, NP_003630, Q91974, AAK72690, NP_032715, NP_055704, CAC83674, and AAK83069.

quences from the EST library were translated and compared to protein sequences already in GenBank by using the BlastX algorithm of the Blastcl3 netclient software (NCBI [ftp://ftp.ncbi.nih.gov/BLAST/blastcl3]) (3). For use in cloning and RACE (rapid amplification of cDNA ends) PCR techniques, total RNA was extracted from 100 juvenile light organs by using the MasterPure complete DNA and RNA purification kit (Epicentre, Madison, WI) according to the manufacturer's protocol. 5′- and 3′-RACE PCR was performed by using the SMART RACE cDNA amplification kit including the Advantage II PCR kit (BD Biosciences, Palo Alto, CA) and the FirstChoice RLM-RACE kit (Ambion, Austin, TX) according to the manufacturers' instructions. 5′- and 3′-RACE-ready cDNA was produced by using 1 μg of symbiotic juvenile light organ mRNA. RACE primers were constructed from the EST sequences identified to have similarity to a transcript of interest. The resulting amplification products were gel purified by using a Geneclean kit (Bio 101, Carlsbad, CA) or the QIAquick gel extraction kit (QIAGEN, Valencia, CA). Purified RACE products were ligated into pGEM-T Easy Vector (Promega, Madison, WI). Calcium-competent cells of *Escherichia coli* DH5α were transformed with the resultant plasmids. Recombinant colonies were screened for the insert of the predicted length, and plasmids were prepared for sequencing by using QIAprep spin miniprep kit columns (QIAGEN). PCR products were sequenced from the recombinant plasmid by using T7 and SP6 primers (Promega, Madison, WI).

Sequence analysis. EST library clones that contained transcripts of interest were fully sequenced. In cases where the EST library clone did not contain the full-length transcript, 5′ or 3′ RACE PCR was used to obtain the complete transcript. For each RACE amplification product, a consensus contiguous sequence was generated by aligning all sequenced clones using MacVector and AssemblyLIGN or the DSgene software package (Accelrys, San Diego, CA), ensuring a three times independent PCR coverage per base. The full sequence of the transcript was determined by (i) the inability of 5′ RACE PCR to amplify any further sequence, coupled with the presence of in-frame stop codons upstream of the prospective methionine start site at the 5′ end, and (ii) the presence of a poly(A) tail following the prospective stop codon at the 3′ end of the transcript. The resulting sequence was analyzed by BLAST searches of GenBank using the default settings (3). Potential open reading frames (ORFs) were predicted by alignment with sequences in GenBank and codon preference analysis (GCG Sequence Analysis; Genetics Computer Group, Inc.). Predicted protein sequences were generated by MacVector or DSgene. The predicted proteins were compared to protein sequences in GenBank by using conserved domain searches within BLAST (44) and SMART (61), secondary structure prediction (Jpred) (14), and alignment. Bootstrapped (1,000 iterations) neighbor-joining trees were constructed based on the Kimura two-parameter correction by using CLUSTAL X (69) with gapped positions included. Maximum-likelihood analyses were also performed on these data using the default parameters of the program proML with global rearrangement in the PHYLIP (version 3.63) suite of programs (22). Trees constructed by the neighbor-joining and maximum-likelihood methods were compared using the Kishino-Hasegawa-Templeton test in proML (38).

RESULTS

Analysis of the EST library showed that the transcriptome of the light organ of *E. scolopes* contains several clusters of transcripts that have high similarity to molecules of the Toll/NF-κB pathway (Table 1 and Fig. 1), including molecules of the receptor complex, signaling molecules, and proteins with high similarity to members of the NF-κB family. The transcripts of genes that are regulated by the Toll/NF-κB pathway in other systems are also present (Table 1 and Fig. 1). With the exception of peptidoglycan recognition protein 3 (PGRP3), the 3′ ESTs are similar to the 3′ region of the most similar molecule in the database, adding to the confidence of their identity. The PGRP3 3′ EST was not found to have sequence similarity with

TABLE 2. Full-length transcripts of *E. scolopes* most similar to key molecules of the Toll/NF-κB pathway[c]

Most similar complete sequence in the database			*E. scolopes* complete sequence		
Protein	Organism[a]	Protein length (aa)	Coding sequence length (aa)	Region of hit[b] (aa)	E value
Receptors					
Toll-like receptor	*Drosophila melanogaster*	1,346	1,191	55–1212	$1e^{-122}$
PGRP1	*Argopecten irradians*	189	207	15–183	$9e^{-42}$
PGRP2	*Argopecten irradians*	189	201	15–183	$4e^{-45}$
PGRP3	*Anopheles gambiae*	188	243	25–187	$7e^{-42}$
PGRP4	*Argopecten irradians*	189	270	15–188	$6e^{-42}$
Signaling molecules					
IRAK4	*Rattus norvegicus*	520	573	1–516	$2e^{-59}$
TRAF6	*Danio rerio*	542	555	53–533	$3e^{-66}$
IKKγ/NEMO	*Homo sapiens*	419	287	154–416	$5e^{-20}$
IκBα	*Rattus norvegicus* p105	1,719	339	1,283–1,473	$2e^{-37}$
NF-κB molecules					
RelA/p65	*Crassostrea gigas* Rel2	614	466	85–475	$4e^{-96}$

[a] *Anopheles gambiae*, mosquito; *Argopecten irradians*, bay scallop; *Crassostrea gigas*, Pacific oyster; *Danio rerio*, zebrafish; *Drosophila melanogaster*, fruit fly; *Homo sapiens*, human; *Rattus norvegicus*, brown rat.

[b] Region of most similar complete sequence in the database that matches the *E. scolopes* complete sequence.

[c] Accession numbers of the most similar complete sequences in the database from the top are as follows: NP_524757, AAR92030, AAR92030, EAA10910, AAR92030, XP_217026, NP_956115, NP_003630, XP_342347, and AAK72691.

sequences in GenBank because it included only a small portion of the ORF. This EST was identified as a candidate PGRP by a BLASTn comparison of *E. scolopes* PGRP1, -2, and -4 against the entire squid 3′ EST database.

Of the 3′ ESTs, ten molecules that are key components of the Toll/NF-κB pathway were investigated further, namely, a Toll-like receptor (TLR), the four PGRPs, interleukin-1 receptor-associated kinase 4 (IRAK4), TNF-α receptor associated factor 6 (TRAF6), inhibitor of κB kinase γ (IKKγ), inhibitor of κB α (IκBα), and REL (Table 2). In all cases, sequencing of the entire coding region improved the similarity to a sequence in the database. However, in the case of Toll, the PGRPs, IRAK4, TRAF6, IκBα, and REL, the best hit to the entire transcript was to the same protein but from a different organism than that of the 3′ EST (Table 2). Trees constructed using the neighbor-joining and maximum likelihood with global rearrangement methods were not found to be statistically different.

TLR. 5′ and 3′ RACE revealed a 4,186-bp transcript that contains an ORF encoding a 1,191-amino-acid (aa) protein (Table 2 and Fig. 2). The conserved regions of the *E. scolopes* Toll-like protein share 26% identity and 46% positive substitutions with Toll-8 from *D. melanogaster*. The predicted Toll-like protein contains a signal peptide, N-terminal leucine-rich repeat (LRR) domains and a C-terminal Toll/IL-1 receptor (TIR) domain (conserved domain search [CDS] E value of $4e^{-13}$) separated by a transmembrane domain. This domain architecture is consistent with the known architecture of previously described Toll-like proteins from both mammals and insects (Fig. 2A and Fig. S1 in the supplemental material). Therefore, the *E. scolopes* Toll-like protein is predicted to be an integral membrane protein with the N terminus on the extracellular membrane face. Because of the inherent variability of the MAMP-recognizing LRR domains in TLRs (8, 51), phylogenetic comparison of Toll-like sequences results in a tree exhibiting long branch lengths. Consequently, the Toll sequences of only relatively recently diverged organisms group together (for example, the TLR3s from vertebrates; Fig. 2B). Therefore, phylogenetic analysis revealed that the *E. scolopes* sequence was not closely associated with any other Toll-like sequence in the database.

PGRPs. Four PGRP transcripts—EsPGRP1, EsPGRP2, EsPGRP3, and EsPGRP4—were identified among the 3′ EST sequences.

(i) EsPGRP1. 5′ and 3′ RACE revealed a 1,362-bp transcript that is predicted to encode a 207-aa protein (Table 2 and Fig. 3A). The putative protein sequence for EsPGRP1 contains a conserved PGRP domain (CDS E value of $1e^{-43}$). Because no other protein domains, such as a signal peptide, were strongly suggested by in silico analysis of the protein structure, EsPGRP1 is predicted to have a cytosolic cellular localization.

(ii) EsPGRP2. 5′ and 3′ RACE results yielded a 949-bp transcript that contains an ORF encoding a 201-aa protein (Table 2 and Fig. 3A). The sequence of EsPGRP2 is very similar to that of EsPGRP1, sharing 82% identity when their coding nucleotide sequences are aligned. At the protein level, EsPGRP1 and EsPGRP2 share 74% identity. The EsPGRP2 protein contains a PGRP domain (CDS E value of $4e^{-48}$). An N-terminal signal peptide sequence is predicted, suggesting that EsPGRP2 is secreted into the extracellular environment, similar to PGRP-SA from *Drosophila melanogaster* (46).

(iii) EsPGRP3. 5′ RACE PCR completed a 2,156-bp EsPGRP3 transcript encoding a 243-aa protein (Table 2 and Fig. 3A). At the nucleotide level EsPGRP3 does not share significant similarity to any of the other EsPGRPs, but the putative EsPGRP3 protein is strongly similar to that of EsPGRP1 and EsPGRP2 (60% identity) with a somewhat weaker similarity to EsPGRP4 (48% identity). EsPGRP3 protein is predicted to have a signal peptide and a PGRP domain (CDS E value of $6.4e^{-68}$). It is also strongly predicted to have a glycosylphosphatidylinositol (GPI)-anchor, which would bind the PGRP to the outer surface of the cell membrane, with a possible GPI-anchor cleavage site at position 216. Therefore,

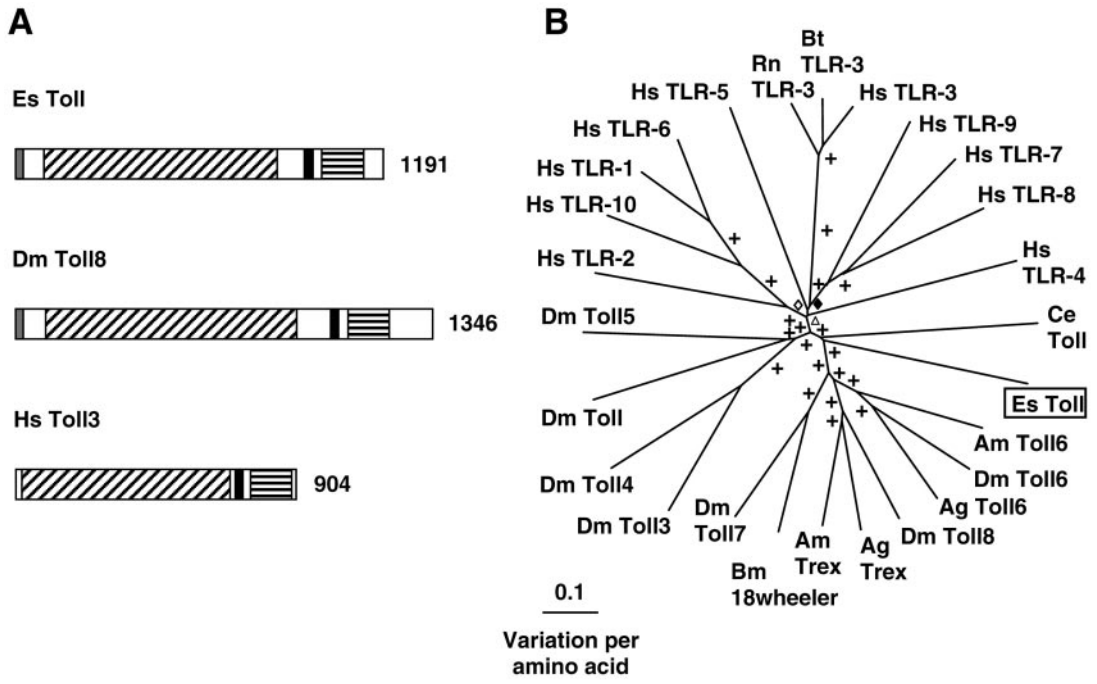

FIG. 2. (A) Comparison of Toll-like receptor proteins from *E. scolopes*, fruit fly, and human. Gray regions indicate the signal peptide, black diagonal shading indicates the LRR region, black regions indicate a transmembrane domain, and black horizontal shading indicates the TIR domain. The number indicates the size of the derived amino acid sequence. Accession numbers are AY956809, NP_524757, and NP_003256, respectively. (B) Unrooted phylogenetic tree produced by the neighbor-joining method, using Kimura two-parameter distances between Toll-like protein sequences of the organisms named on the tree. Gapped positions were included in the analysis. Symbols on the branches represent percentage bootstrap values: +, 90 to 100%; ◇, 80 to 89%; ◆, 70 to 79%; △, 60 to 69%. Accession numbers clockwise from *E. scolopes* are as follows: AY956809, XP_393712, AAF86226, AAL37902, NP_524757, AAL37904, XP_393713, BAB85498, AAF86225, NP_649719, NP_523519, NP_733166, AAF86227, NP_003255, NP_112218, NP_003254, NP_006059, NP_003259, NP_942086, NP_001008664, NP_003256, NP_059138, AAF78035, NP_057694, NP_612564, and AAK37544. Abbreviations: Ag, *Anopheles gambiae* (mosquito); Am, *Apis mellifera* (honeybee); Bm, *Bombyx mori* (silk moth); Bt, *Bos taurus* (cow); Ce, *Caenorhabditis elegans* (nematode); Dm, *Drosophila melanogaster* (fruit fly); Es, *Euprymna scolopes* (Hawaiian bobtail squid); Hs, *Homo sapiens* (human); Rn, *Rattus norvegicus* (rat).

we predict that EsPGRP3 is an extracellular extrinsic membrane protein that may be released into the extracellular environment through cleavage of the GPI-anchor.

(iv) EsPGRP4. The 5′ and 3′ RACE PCR product sequence indicated that the EsPGRP4 transcript is 1,527 bp encoding a 270-aa protein (Table 2 and Fig. 3A). At the nucleotide level, the coding sequence of EsPGRP4 does not share significant similarity to either EsPGRP1 or EsPGRP2 (using the BLASTn algorithm). The EsPGRP4 protein sequence is about 45 and 52% identical to EsPGRP1 and EsPGRP2, respectively. EsPGRP4 contains a putative PGRP domain (CDS E value of $1e^{-42}$). The prediction of two N-terminal transmembrane domains suggests that EsPGRP4 is an integral membrane protein.

When the *E. scolopes* PGRPs (EsPGRPs) are compared to PGRP molecules from other organisms (Fig. 3B), the *E. scolopes* molecules group together with strong bootstrap support (>70%). Apart from this cluster and the cluster containing the PGRP-LD and PGRP-LAa from *D. melanogaster*, there is no other strong bootstrap support for the PGRPs of a single organism grouping together. EsPGRPs also did not group with a PGRP from another mollusk, *Argopecten irradians* (the bay scallop). These data suggest that the PGRPs identified from the *E. scolopes* light organ were derived from a single ancestral EsPGRP. Such findings do not preclude the possibility of other EsPGRPs that would cluster outside of those already found, and are derived from a different PGRP.

Some PGRPs have T7 lysozyme-like catalytic activity, including PGRP-LB from *D. melanogaster* (37, 45), which coordinates a zinc ion required for *N*-acetylmuramic acid L-alanine amidase (NAMLAA) activity with a conserved tetrad of two histidines, a critical cysteine, and tyrosine residue (H42, Y78, H152, and C160, PGRP-LB numbering). EsPGRP1, EsPGRP2, and EsPGRP3 contain all four zinc coordinating residues in the PGRP-binding domain, suggesting zinc-dependent NAMLAA activity in these three proteins (Fig. 3C). At the homologous position of the critical cysteine 160, EsPGRP4 contains a serine substitution similar to *D. melanogaster* PGRP-SA, which does not coordinate a zinc ion in the binding pocket (56). It is likely that EsPGRP4 does not act as a catalytic PGRP and is limited to PGN recognition and/or signal transduction functions. All four EsPGRPs contain a pair of cysteines C50 and C56 (using PGRP-LB numbering) at synonymous positions with those essential for the structure of the PGN binding pocket and a highly conserved threonine, T158 (using PGRP-LB numbering) that is required in the binding of PGN by PGRP-LB from *D. melanogaster* (37).

IRAK4. 5′ and 3′ RACE PCR of juvenile light organ RNA resulted in a 1,791-bp transcript that contains an ORF encoding a 537-aa protein (Table 2 and Fig. 4). The translated

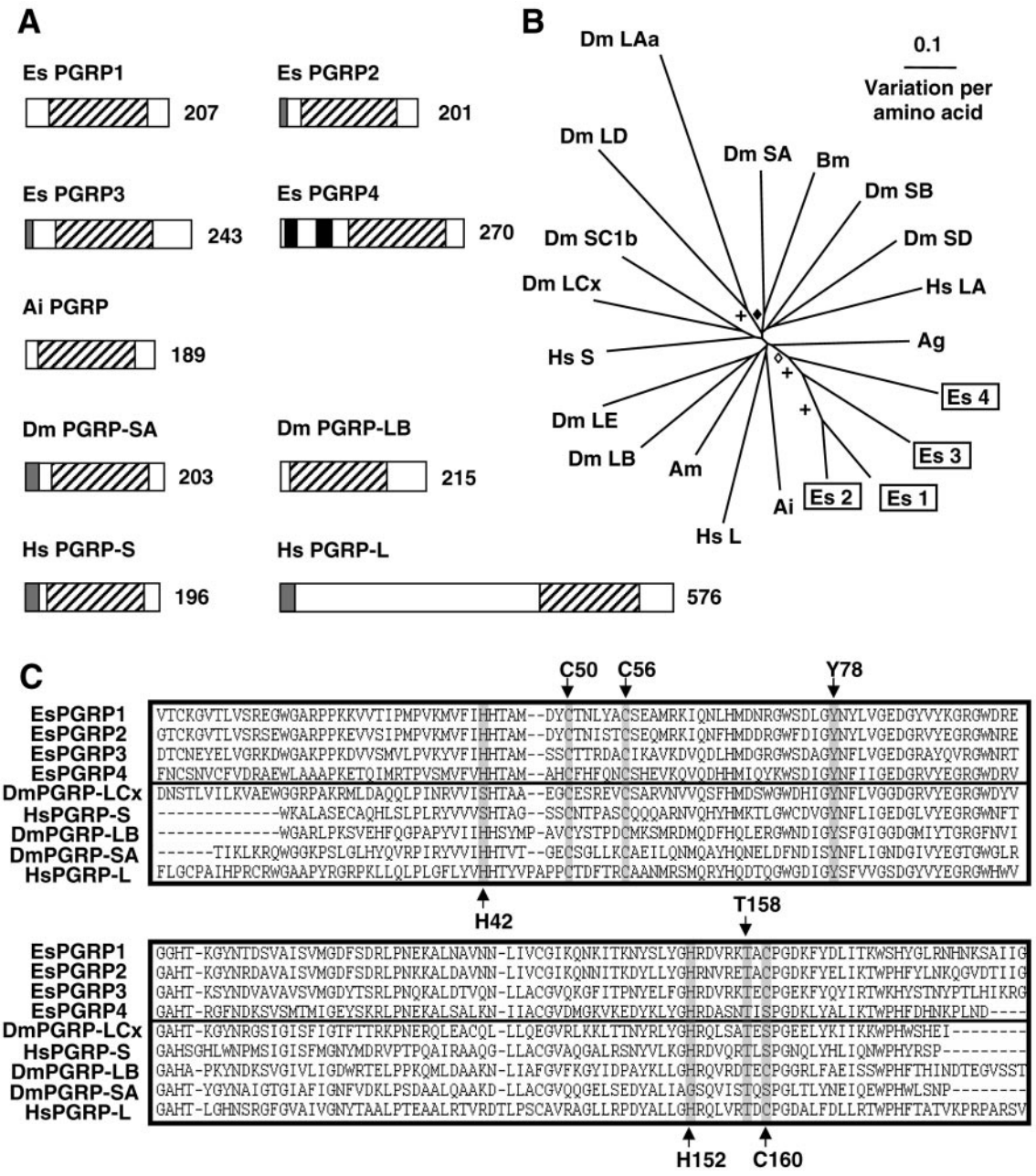

FIG. 3. (A) Comparison of PGRP proteins from *E. scolopes*, bay scallop, fruit fly, and human sources. Gray regions indicate the signal peptide, black regions indicate a transmembrane domain, and black diagonal shading indicate the PGRP domain. The number indicates the size of the derived amino acid sequence. Reading from left to right and down from the top, accession numbers are AY956811, AY956812, AY956813, AY956814, AAR92030, NP_572727, NP_731576, NP_005082, and AAL05629, respectively. (B) Unrooted phylogenetic tree produced by the neighbor-joining method, using Kimura two-parameter distances between PGRP protein sequences of the organisms named on the tree. Gapped positions were included in the analysis. Symbols on the branches represent percentage bootstrap values: +, 90 to 100%; ◇, 80 to 89%; ◆, 70 to 79%. Values below 70% are not shown. Accession numbers clockwise from *E. scolopes* PGRP1 are as follows: AY956811, AY956812, AAR92030, AAL05629, XP_395941, NP_731576, AAG32064, NP_005082, NP_729468, AAG23736, NP_788467, AAK00295, NP_572727, BAA77210, CAD89136, CAD89193, NP_443123, EAA10910, AY956814, and AY956813. (C) Alignment of the PGRP domains of the EsPGRPs and those of other organisms. Residues critical to PGRP function are highlighted. Accession numbers from top to bottom are as follows: AY956811, AY956812, AY956813, AY956814, NP_729468, NP_005082, NP_731576, NP_572727, and AAL05629. Abbreviations: Ag, *Anopheles gambiae* (mosquito); Ai, *Argopecten irradians* (bay scallop); Am, *Apis mellifera* (honeybee); Bm, *Bombyx mori* (silk moth); Dm, *Drosophila melanogaster* (fruit fly); Es, *Euprymna scolopes* (Hawaiian bobtail squid); Hs, *Homo sapiens* (human).

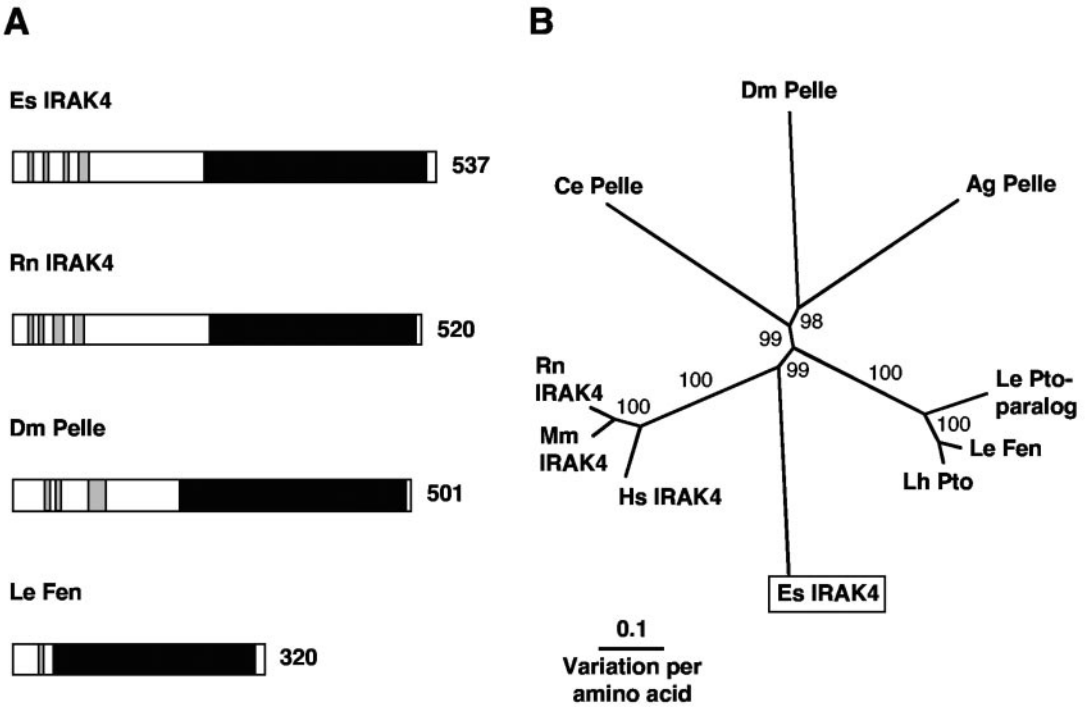

FIG. 4. (A) Comparison of IRAK4-like proteins from *E. scolopes*, rat, fruit fly, and tomato. Black regions indicate the serine/threonine protein kinase domain, and gray regions indicate the alpha helices of a possible death domain. Number indicates size of the derived amino acid sequence. The accession numbers are AY956810, XP_217026, NP_476971, and T07416, respectively. (B) Unrooted phylogenetic tree produced by the neighbor-joining method, using Kimura two-parameter distances between IRAK4 protein sequences of the organisms named on the tree. Gapped positions were included in the analysis. The numbers on the branches are percent bootstrap values. Accession numbers clockwise from *E. scolopes* are as follows: AY956810, NP_057207, NP_084202, XP_217026, NP_502587, NP_476971, XP_311931, AAF76311, T07416, and AAK11568. Abbreviations: Ag, *Anopheles gambiae* (mosquito); Ce, *Caenorhabditis elegans* (nematode); Dm, *Drosophila melanogaster* (fuit fly); Es, *Euprymna scolopes* (Hawaiian bobtail squid); Hs, *Homo sapiens* (human); Le, *Lycopersicon esculentum* (tomato); Lh, *Lycopersicon hirsutum* (tomato); Mm, *Mus musculus* (mouse); Rn, *Rattus norvegicus* (rat).

transcript exhibited a C-terminal serine/threonine protein kinase domain (CDS E value of $5e^{-34}$) and at least four N-terminal α-helices of a possible death domain (31), characteristic of IRAK proteins (Fig. 4A and Fig. S2 in the supplemental material). When the *E. scolopes* IRAK4 is compared to IRAK4-like molecules from other organisms, the *E. scolopes* molecule clusters with the vertebrate IRAK4 protein sequences with strong bootstrap support (Fig. 4B). However, the branch lengths within this cluster indicate that the *E. scolopes* sequence is separate from the vertebrate IRAK4 cluster.

TRAF6. 5′ and 3′ RACE resulted in a 2,019-bp transcript that contains an ORF encoding a 555-aa protein (Table 2 and Fig. 5). The derived amino acid sequence of the *E. scolopes* transcript has a number of characteristic TRAF domains (64) (Fig. 5A and Fig. S3 in the supplemental material). All TRAF proteins share a common C-terminal TRAF domain (CDS E value of $7e^{-42}$) required for the interaction with upstream factors such as IRAK4 (12). The putative protein also contains two TRAF-type zinc-finger domains (CDS E value of $2e^{-7}$) N-terminal to the TRAF domain and a RING finger motif (CDS E value of e^{-7}) at its extreme N terminus. The N-terminal region of TRAF6 and especially the RING finger motif are required for efficient IKK and NF-κB activation (7, 12, 15). Comparison of the *E. scolopes* sequence with TRAF sequences from other organisms supports its classification as TRAF6 (Fig. 5B). *E. scolopes* TRAF6 clusters with the vertebrate TRAF6 sequences with strong bootstrap support. *E. scolopes* TRAF6 is 33% similar to human TRAF6, whereas only sharing similarities of 26, 28, 26, and 29% to TRAF2, TRAF3, TRAF4, and TRAF5 of humans, respectively. TRAF-like proteins from *D. melanogaster* and *A. gambiae* branch one node away from TRAF6 of *E. scolopes* and vertebrates, and this grouping is also well supported. The branch lengths indicate that *E. scolopes*, vertebrates, and insects are separate from each other within the TRAF6-like sequence cluster.

IKKγ. 5′ and 3′ RACE PCR amplified a 2,323-bp transcript that contains an ORF encoding a 431-aa protein (Table 2 and Fig. 6). Identification of IKKγ proteins requires secondary structure analysis, as opposed to conserved domain searches, because IKKγ proteins do not contain unique IKKγ domains. IKKγ proteins are predominantly helical with large stretches of coiled-coil structure, including a leucine zipper motif and a zinc finger motif at the C terminus (35, 57). These motifs are likely to be involved in protein-protein interactions. Secondary structure analysis of the derived amino acid sequence (Fig. 6A and Fig. S4 in the supplemental material) indicates that the *E. scolopes* protein is a canonical IKKγ (35, 57). Similarly, the *E. scolopes* sequence clusters with IKKγ proteins of vertebrates with strong bootstrap support, although the branch lengths

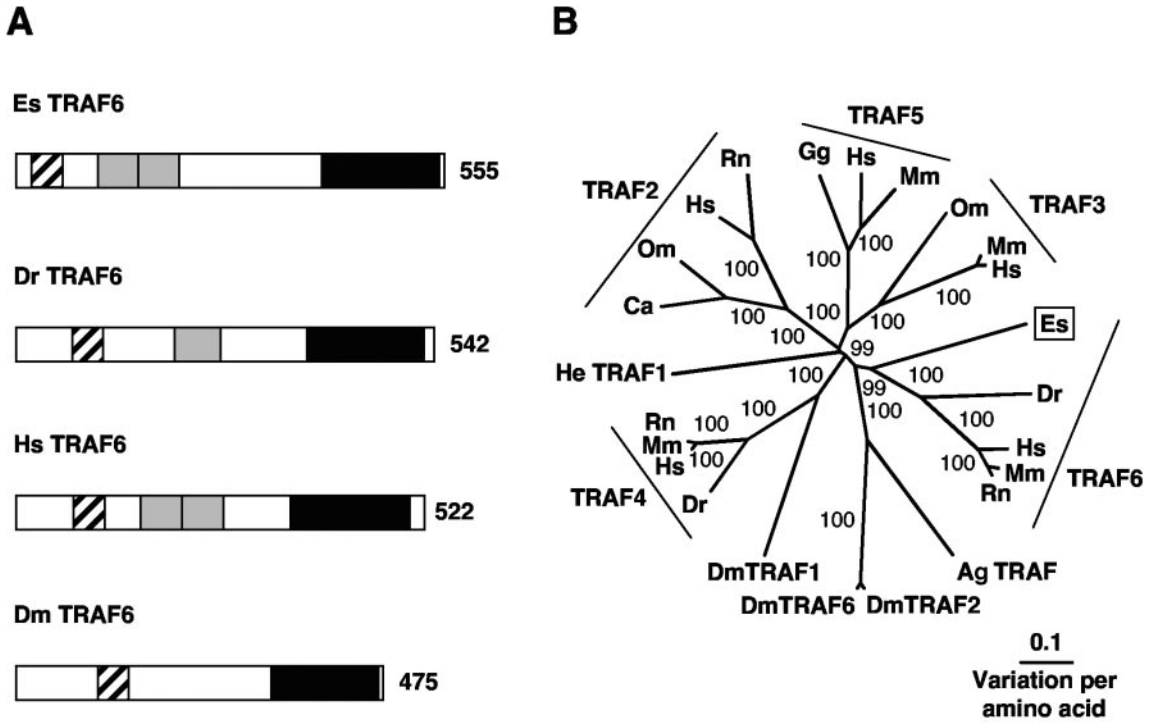

FIG. 5. (A) Comparison of TRAF6 proteins from *E. scolopes*, zebrafish, human, and fruit fly with characteristic domains indicated. Black hatched shading indicates the RING finger domain, gray regions indicate the TRAF-type zinc finger domains, and black regions indicate the TRAF homology domain. The number indicates size of the derived amino acid sequence. The accession numbers are AY956816, NP_956115, NP_004611, and AAD47895, respectively. (B) Unrooted phylogenetic tree produced by the neighbor-joining method, using Kimura two-parameter distances between TRAF protein sequences of the organisms named on the tree. Gapped positions were included in the analysis. Numbers on the branches are percentage bootstrap values. Accession numbers clockwise from *E. scolopes* are as follows: AY956816, NP_956115, NP_004611, P70196, XP_230377, XP_311879, AAD34345, AAD47895, AAD34346, NP_991325, NP_004286, NP_033449, XP_220640, CAE88928, CAC82653, CAD69021, NP_066961, XP_231032, NP_989550, NP_004610, NP_035763, CAD57164, NP_035762, and Q13114. Abbreviations: Ag, *Anopheles gambiae* (mosquito); Ca, *Carassius auratus* (goldfish); Dm, *Drosophila melanogaster* (fruit fly); Dr, *Danio rerio* (zebrafish); Es, *Euprymna scolopes* (Hawaiian bobtail squid); Gg, *Gallus gallus* (chicken); He, *Hydractinia echinata* (hydrozoa); Hs, *Homo sapiens* (human); Mm, *Mus musculus* (mouse); Om, *Oncorhynchus mykiss* (rainbow trout); Rn, *Rattus norvegicus* (rat).

indicate the derived amino acid sequence of *E. scolopes* is separate from the vertebrate sequences (Fig. 6B). IKKγ from *D. melanogaster* branches one node away and is separated by a long branch from IKKγ of *E. scolopes* and vertebrates. The insect, vertebrate, and mollusk proteins form a well-supported IKKγ grouping that is separate from IKKα and IKKβ sequences.

IκB. 5′ and 3′ RACE resulted in a 1,463-bp transcript that contains an ORF encoding a 339-aa protein (Table 2 and Fig. 7). Similar to other IκB family members, the derived amino acid sequence exhibited six ankyrin repeat domains (CDS E value of $9e^{-23}$), an N-terminal regulatory region, and a C-terminal region rich in Pro, Glu/Asp, Ser, and Thr residues (PEST-rich region) (Fig. 7A and Fig. S5 in the supplemental material). Proteins of the IκB family contain either six or seven ankyrin repeats that mediate binding to the REL homology domain and mask the nuclear localization signal of REL family proteins (35). The N-terminal regulatory region is required for stimulus-induced degradation of the protein, the key step in NF-κB activation. Only the "professional" IκBs (74), namely, IκBα, IκBβ, IκBε, and Cactus, contain this short peptide stretch centered around two serine residues that can be inducibly phosphorylated (35). Mutations at either serine residue of this region results in the stabilization of the protein (6, 50, 74). The presence of this N-terminal regulatory region, coupled with the inability of 5′ RACE PCR to amplify any further sequence and in-frame stop codons upstream of the prospective start site, provides evidence that the sequence is complete and is not the C terminus of a p105-like or RELISH-like transcript that also has IκB-like characteristics (27, 41, 64). However, the sequence of the regulatory region in the *E. scolopes* protein has a conserved substitution in the third position, i.e., instead of the DSGXXS characteristic of the vertebrate IκBs and the drosophila homolog Cactus, the sequence of this region of the *E. scolopes* IκB is DSAXXS. The ubiquitin conjugation site, a lysine residue located 9 to 12 aa N-terminal to the recognition site of professional IκB is, however, shared by the *E. scolopes* sequence (74). The C-terminal contains a PEST-rich region. PEST sequences are often found in proteins with a rapid turnover rate and may be necessary for the degradation of IκB. For example, in mouse cell lines that were transfected with human IκBα missing the final 41 aa, including the PEST sequence, the mutant IκBα was phosphorylated but not degraded (11). The *E. scolopes* sequence clustered with IκBα-like proteins (Fig. 7B). Within this IκBα cluster, the putative protein sequence from *E. scolopes* did not group with either

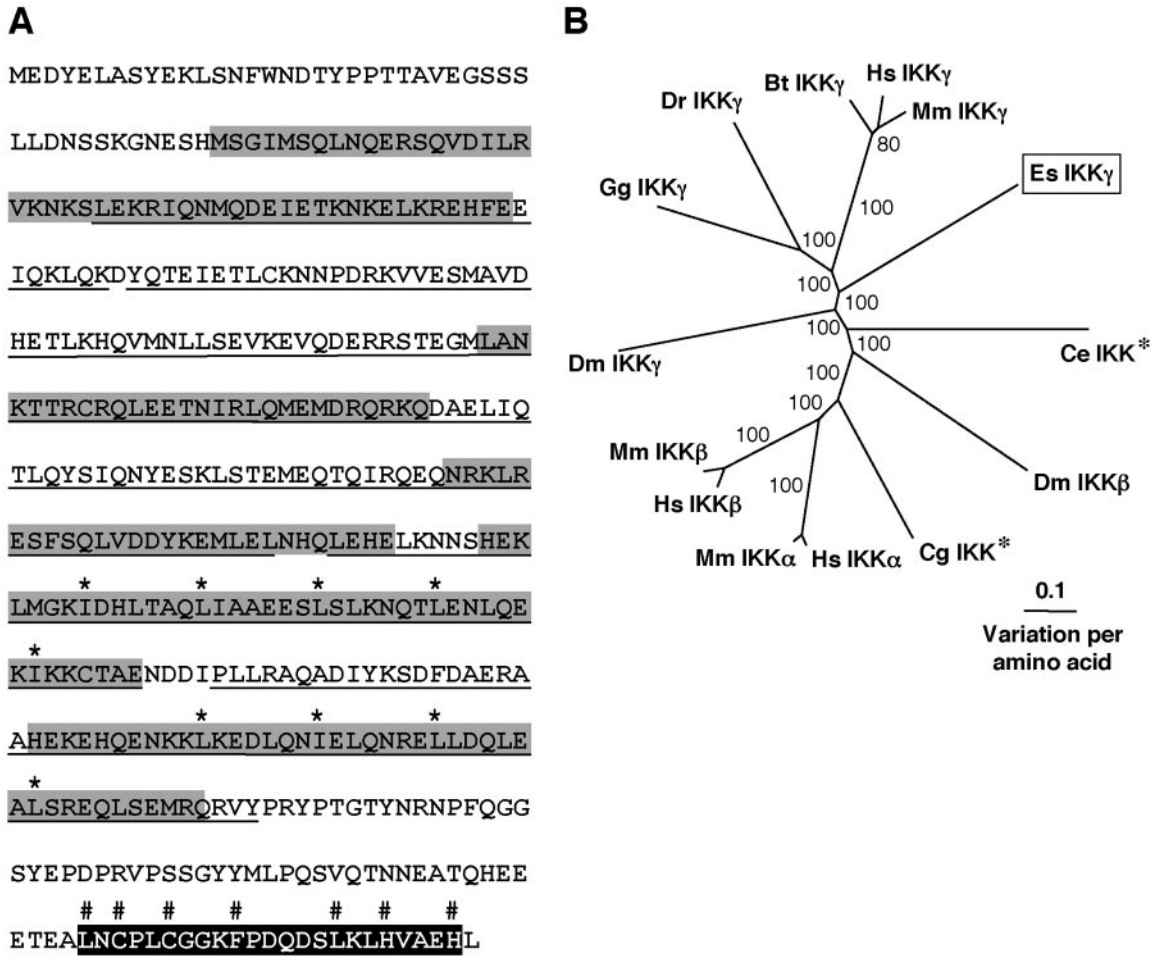

FIG. 6. (A) The characteristic domains of IKKγ exhibited by the derived amino acid sequence from *E. scolopes*. The underlined region represents a helical structure containing coiled coil regions (gray shading) and a leucine zipper motif with specific leucines (and hydrophobic isoleucine) marked with an asterisk. The C-terminal zinc finger motif is shaded in black with characteristic amino acids labeled with a "#" symbol. (B) Unrooted phylogenetic tree produced by the neighbor-joining method, using Kimura two-parameter distances between IKK protein sequences of the organisms named on the tree. Gapped positions were included in the analysis. Numbers on the branches are percentage bootstrap values. *, The original description does not indicate assignment to α, β, or γ classes of IKK. Accession numbers clockwise from *E. scolopes* are as follows: AY956817, NP_499831, AAG02485, AAC05683, NP_001269, AAH18243, NP_001547, NP_034676, AAG02486, NP_989567, AAH63986, NP_776779, NP_003630, and AAM54725. Abbreviations: Bt, *Bos taurus* (cow); Ce, *Caernorhabditis elegans* (nematode); Cg, *Crassostrea gigas* (Pacific oyster); Dm, *Drosophila melanogaster* (fruit fly); Dr, *Danio rerio* (zebrafish); Es, *Euprymna scolopes* (Hawaiian bobtail squid); Gg, *Gallus gallus* (chicken); Hs, *Homo sapiens* (human); Mm, *Mus musculus* (mouse).

D. melanogaster Cactus or vertebrate IκBα proteins with strong bootstrap support, and branch lengths indicated that the vertebrates, *D. melanogaster*, and *E. scolopes* sequences were distinct from each other (Fig. 7B).

REL. 5′ and 3′ RACE of light organ RNA resulted in a 1,557-bp transcript that contains an ORF encoding a 466-aa protein (Table 2 and Fig. 8). The derived amino acid sequence of the transcript exhibited a REL homology domain (RHD), containing an immunoglobulin-like plexin domain (CDS E value of $3e^{-35}$) and a conserved nuclear localization motif (Fig. 8A and Fig. S6 in the supplemental material). The RHD (CDS E value of $5e^{-62}$) is characteristic of REL family transcription factors and is responsible for dimerization, DNA-binding via the conserved motif RXXRXRXXC and interaction with IκB (35). The transactivation domain, C-terminal of the RHD, is less well-conserved and is thought to be involved in the activation of transcription (41). No regions that are critical for transcriptional activation have been identified within the transactivation domain, apart from the presence of the transactivation domain itself (26, 27, 41, 47). The REL family of proteins can be separated into two distinct classes: class I contains the precursor REL proteins with C-terminal domains that have IκB-like characteristics, such as vertebrate and insect p100, p105, and Relish; class II contains the NF-κB subunit REL proteins, including p65/RelA, RelB, c-REL, v-Rel, and Dorsal (27). Compared to the other class II REL proteins, the *E. scolopes* REL sequence is relatively short (Fig. 8A). The difference appears to be in the length of the transactivation domain, since the size of the RHD of both proteins is similar. Since there is a 3′ stop codon and 3′ RACE PCR failed to amplify any sequence further 3′ of the poly(A) tail and, since the transactivation domain is known to be less

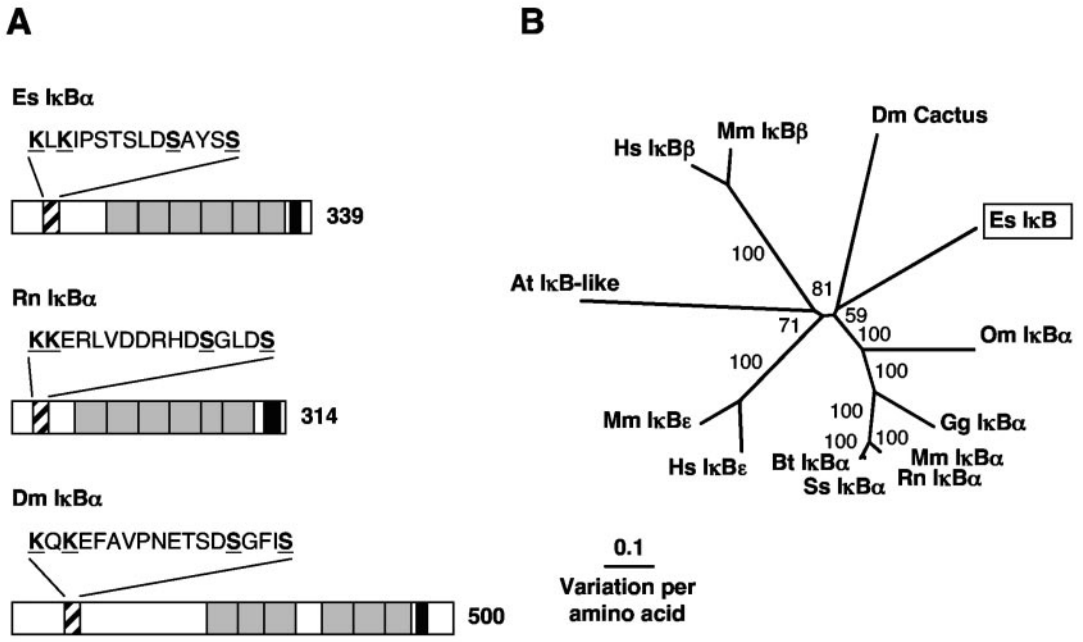

FIG. 7. (A) Comparison of IκB family molecules from *E. scolopes*, rat, and fruit fly. Black diagonal shading represents the N-terminal regulatory region, with the serines of the phosphorylation site and the lysines of the possible ubiquitin conjugation sites underlined and highlighted in boldface. The ankyrin repeat domains are shaded in gray, and the PEST-rich region is shaded in black. The number indicates the size of the derived amino-acid sequence. The accession numbers are AY956818, XP_343066, and NP_476942, respectively. (B) Unrooted phylogenetic tree produced by the neighbor-joining method, using Kimura two-parameter distances between IκB protein sequences of the organisms named on the tree. Gapped positions were included in the analysis. The numbers on the branches are percent bootstrap values. The accession numbers clockwise from *E. scolopes* are as follows: AY956818, CAC85086, Q91974, NP_035037, XP_343066, Q08353, CAD12786, O00221, NP_032716, AAB58262, NP_002494, NP_035038, and NP_476942. Abbreviations: At, *Arabidopsis thaliana* (thale cress); Bt, *Bos taurus* (cow); Dm, *Drosophila melanogaster* (fruit fly); Es, *Euprymna scolopes* (Hawaiian bobtail squid); Gg, *Gallus gallus* (chicken); Hs, *Homo sapiens* (human); Mm, *Mus musculus* (mouse); Om, *Oncorhynchus mykiss* (rainbow trout); Rn, *Rattus norvegicus* (rat); Ss, *Sus scrofa* (pig).

conserved, we conclude that the sequence is complete. Compared to class II REL proteins from other organisms, the *E. scolopes* sequence clusters with the *Crassostrea gigas* REL sequences with strong bootstrap support (Fig. 8B). Since the insects and the vertebrate class II REL proteins, respectively, also form groupings that are strongly supported and the branch lengths separating the sequences are long, it is concluded that the mollusk sequences are distinct from the vertebrate and insect class II REL proteins.

DISCUSSION

The results of our analyses provide evidence for the presence of several transcripts encoding components of the Toll/NF-κB pathway in *E. scolopes*, including receptors, signal transducers, and targets of the pathway (Fig. 9). Although this pathway appears to be present, its characteristics suggest certain unique features. This finding is not surprising, since *E. scolopes* is phylogenetically distant from the other animals for which this pathway has been described in detail.

Beginning with the receptors, only one TLR was identified in the EST library. This finding was surprising since multiple Tolls and TLRs have been identified in the insects and vertebrates, respectively (9, 68). The light organ may only express a single TLR gene that may be a global, rather than a specific, microbe receptor, although it is possible that other TLR candidates were not recognized from the 3′ EST library. The large genome size of *E. scolopes* (3.7Gb; T. R. Gregory, Animal Genome Size Database [http://www.genomesize.com]) and the inherent difficulties with working with cephalopod DNA (62, 66) have thus far precluded us from performing reliable Southern blots and genomic DNA amplification to identify any other TLRs. In contrast, several PGRPs were identified, but analyses of the *E. scolopes* PGRPs revealed that they do not readily fall into the classes of PGRPs identified in insect and mammals (19, 42, 72). Most notably, unlike the PGRPs of other animals, all of the EsPGRPs that we have identified thus far occur in a well-supported group, suggesting that this cohort of proteins was derived from a single ancestral PGRP. Further, the sequence data and structure predictions of the EsPGRPs do not support the classification of these proteins by their biochemical characteristics in the same ways that have been applied to other PGRPs. For example, the characteristics of molecular mass, as well as the patterns of occurrence of signal sequences and transmembrane domains, do not group the EsPGRPs into distinct classes as they do in the insects (72). Because each of the EsPGRPs is predicted to have unique biochemical characteristics, it is likely that they have distinct functions. The finding of four EsPGRPs in the light organ does not preclude the possibility that others exist there or in other parts of the body.

Within the pathway, several elements critical for MAMP-induced triggering of the NF-κB pathway were identified, including IRAK4, TRAF6, IKKγ, IκB-like, and REL-like transcripts (17, 25, 35, 43, 57, 64, 67, 73). In another mollusk,

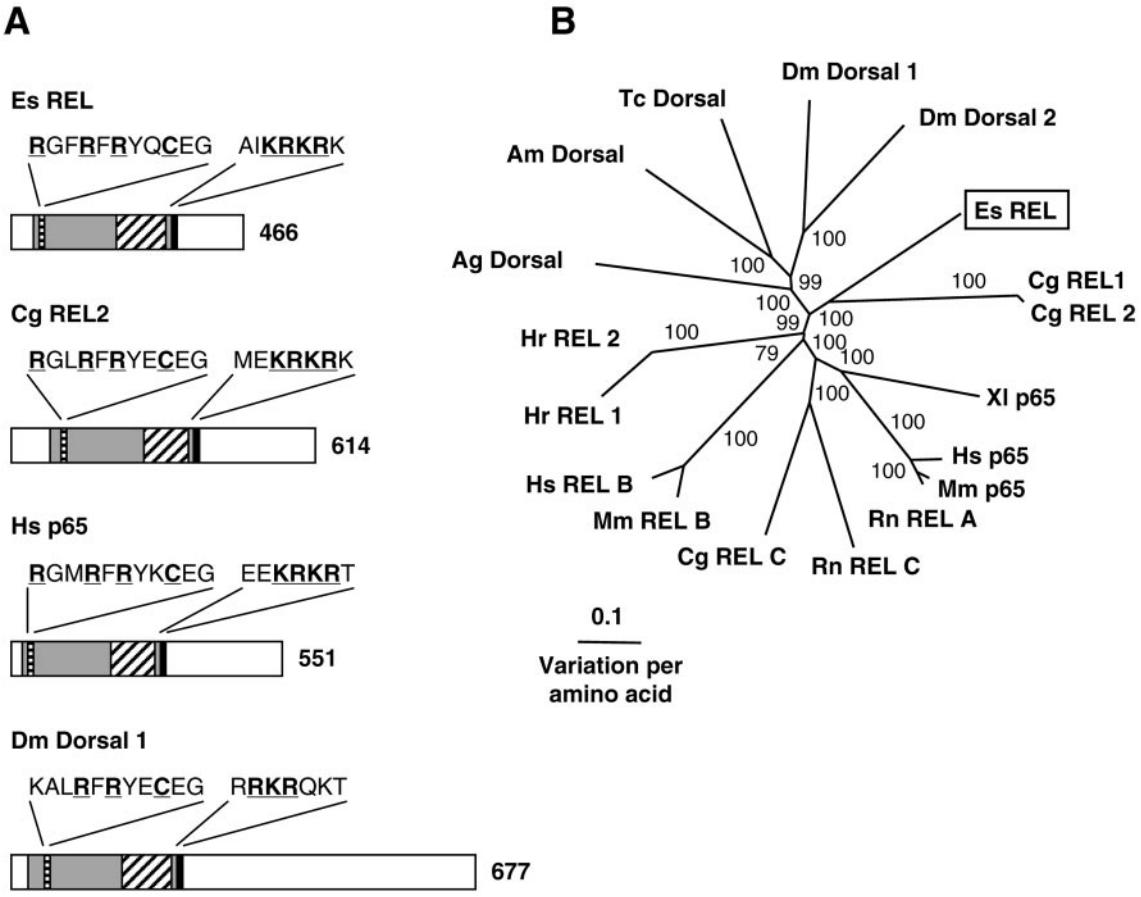

FIG. 8. (A) Comparison of REL family proteins from *E. scolopes*, oyster, human, and fruit fly. The RHD is indicated by gray shading and contains the following: the conserved residues of the DNA-binding motif (black horizontal shading) underlined and highlighted in boldface; the immunoglobulin-like plexin domain, found in all REL family molecules, indicated by black diagonal shading; and the nuclear localization signal indicated by solid black shading, with conserved residues underlined and highlighted in boldface. The unshaded region that is C-terminal to the RHD represents the transactivation domain. The number indicates size of the derived amino acid sequence. Accession numbers are AY956819, AAK72691, NP_068810, and NP_724052, respectively. (B) Unrooted phylogenetic tree produced by the neighbor-joining method, using Kimura two-parameter distances between REL protein sequences of the organisms named on the tree. Gapped positions were included in the analysis. Numbers on the branches are percentage bootstrap values. Accession numbers clockwise from *E. scolopes* are as follows: AY956819, AAK72690, AAK72691, Q04865, NP_068810, NP_033071, XP_238994, XP_223688, P16236, NP_033072, Q01201, BAB47172, BAB47173, XP_310177, AAP23055, AAG22858, NP_724052, and NP_724054. Abbreviations: Ag, *Anopheles gambiae* (mosquito); Am, *Apis mellifera* (honeybee); Cg, *Crassostrea gigas* (Pacific oyster); Dm, *Drosophila melanogaster* (fruit fly); Es, *Euprymna scolopes* (Hawaiian bobtail squid); Hr, *Halocynthia roretzi* (ascidian); Hs, *Homo sapiens* (human); Mm, *Mus musculus* (mouse); Rn, *Rattus norvegicus* (rat); Tc, *Tribolium castaneum* (beetle); XI, *Xenopus laevis* (African clawed frog).

Crassostrea gigas (the Pacific oyster), full-length transcripts of an IKK (20), which appears to be an IKKβ, and a REL-like protein (48) were identified, lending further support for the presence of the pathway in the mollusks. An element not identified in the *E. scolopes* EST database was a MyD88-like transcript, which in other systems encodes a critical protein that links the Toll-like receptor to the IRAK protein. However, a partial sequence of a molluscan MyD88-like transcript has been identified in *C. gigas* (28), suggesting that *E. scolopes* may have this gene, although it may not be expressed at high levels in the light organ. Attempts to identify this transcript in other *E. scolopes* tissues by reverse transcription-PCR amplification were not successful.

The transcripts described in the present study can be used to propose a putative Toll/NF-κB signaling pathway in *E. scolopes* (Fig. 9). Taken together, the data for *E. scolopes* and the distantly related *C. gigas* provide strong evidence that this pathway is likely to occur throughout the Phylum Mollusca, as well as across the entire superphylum containing the mollusks, i.e., the Lophotrochozoa. The phylogenetic trees for the *E. scolopes* proteins do not clarify whether the *E. scolopes* sequences group closer to the vertebrates or the insects, although most of the closest BLAST hits are to vertebrate sequences. The relationship among the superphyla of the animals is controversial, with most phylogenies aligning the Lophotrochozoa with the Ecdysozoa, rather than the Deuterostomia (59). Further analysis of the *E. scolopes* EST library and those of other Lophotrochozoa will be necessary to address this issue rigorously.

The complex patterns of bacteria-induced development in

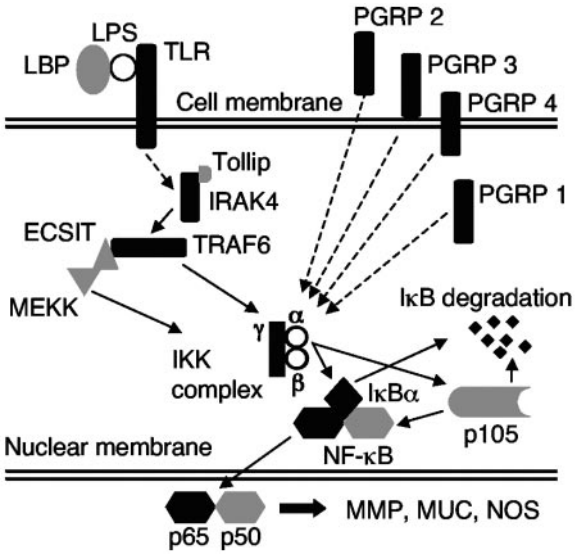

FIG. 9. Putative signaling pathway of the evolutionarily conserved Toll/NF-κB pathway utilizing the *E. scolopes* transcripts identified in the present study. Black shading indicates identification of full-length transcripts, and gray shading indicates identification of partial length transcripts (see Tables 1 and 2). Dashed lines indicate a pathway in which not all of the signaling intermediates have been found in *E. scolopes*.

the squid light organ, along with the different functions of MAMPs in the process, suggest that the NF-κB pathway may be modulated differently over time and in location through the early development of the light organ. The high levels of nitric oxide synthase (NOS) (16) and the mucus shedding (52, 54) in response to environmental PGN would be consistent with activity of the pathway in the superficial field of ciliated cells during the initial phases of colonization. However, nitric oxide/NOS levels are attenuated (16), mucus shedding ceases (52), and apoptosis (24) is induced in this field of cells by the subsequent interactions of the host and symbiont within the crypt space, which is several cell layers away. These observations suggest that remote signaling by the symbionts may turn down the activity of the pathway in the superficial field of ciliated cells. In contrast, the MAMPs responsible for development, i.e., derivatives of PGN and LPS, are presented directly to the crypt cells. These receptor-ligand interactions may increase the activity of the pathway in the cells with which the bacteria directly interact. In support of this possibility is the observation that mucus shedding by the crypt cells results from colonization of the crypts with symbionts (52).

The data presented here demonstrate the presence of the NF-κB pathway in the *E. scolopes* light organ, and the patterns of development and the involvement of MAMPs provide circumstantial evidence for its activity during the onset of the symbiosis. A full understanding of the connection among these findings awaits an in-depth analysis of the activity of the pathway in the various tissues of the light organ.

ACKNOWLEDGMENTS

We thank W. Crookes-Goodson and A. Wier for helpful discussion and comments on the manuscript.

This research was supported by a grant from the W. M. Keck Foundation (to E. P. Greenberg and M.M.-N.), by NSF grant IBN 0451102 (to M.M.-N. and E. G. Ruby), by NIH grant AI 50611 (to M.M.-N.), by NIH grant RR12294 (to E. G. Ruby and M.M.-N.), and by a Career Development Award from Research to Prevent Blindness (to T.E.S).

REFERENCES

1. **Aderem, A., and R. J. Ulevitch.** 2000. Toll-like receptors in the induction of the innate immune response. Nature **406:**782–787.
2. **Aguinaldo, A. M., J. M. Turbeville, L. S. Linford, M. C. Rivera, J. R. Garey, R. A. Raff, and J. A. Lake.** 1997. Evidence for a clade of nematodes, arthropods and other moulting animals. Nature **387:**489–493.
3. **Altschul, S. F., W. Gish, W. Miller, E. W. Myers, and D. J. Lipman.** 1990. Basic local alignment search tool. J. Mol. Biol. **215:**403–410.
4. **Anton, P. M., V. Theodorou, S. Roy, J. Fioramonti, and L. Bueno.** 2002. Pathways involved in mild gastrointestinal inflammation induced by a low level exposure to a food contaminant. Dig. Dis. Sci. **47:**1308–1315.
5. **Asai, T., G. Tena, J. Plotnikova, M. R. Willmann, W. L. Chiu, L. Gomez-Gomez, T. Boller, F. M. Ausubel, and J. Sheen.** 2002. MAP kinase signalling cascade in *Arabidopsis* innate immunity. Nature **415:**977–983.
6. **Baldwin, A. S., Jr.** 1996. The NF-κB and IκB proteins: new discoveries and insights. Annu. Rev. Immunol. **14:**649–683.
7. **Baud, V., Z. G. Liu, B. Bennett, N. Suzuki, Y. Xia, and M. Karin.** 1999. Signaling by proinflammatory cytokines: oligomerization of TRAF2 and TRAF6 is sufficient for JNK and IKK activation and target gene induction via an amino-terminal effector domain. Genes Dev. **13:**1297–1308.
8. **Bell, J. K., G. E. Mullen, C. A. Leifer, A. Mazzoni, D. R. Davies, and D. M. Segal.** 2003. Leucine-rich repeats and pathogen recognition in Toll-like receptors. Trends Immunol. **24:**528–533.
9. **Beutler, B.** 2004. Inferences, questions and possibilities in Toll-like receptor signalling. Nature **430:**257–263.
10. **Boettcher, K. J., and E. G. Ruby.** 1990. Depressed light emission by symbiotic *Vibrio fischeri* of the sepiolid squid *Euprymna scolopes.* J. Bacteriol. **172:**3701–3706.
11. **Brown, K., S. Gerstberger, L. Carlson, G. Franzoso, and U. Siebenlist.** 1995. Control of IκBα proteolysis by site-specific, signal-induced phosphorylation. Science **267:**1485–1488.
12. **Cao, Z., W. J. Henzel, and X. Gao.** 1996. IRAK: a kinase associated with the interleukin-1 receptor. Science **271:**1128–1131.
13. **Clifton, D. R., R. A. Goss, S. K. Sahni, D. van Antwerp, R. B. Baggs, V. J. Marder, D. J. Silverman, and L. A. Sporn.** 1998. NF-κB-dependent inhibition of apoptosis is essential for host cell survival during *Rickettsia rickettsii* infection. Proc. Natl. Acad. Sci. USA **95:**4646–4651.
14. **Cuff, J. A., M. E. Clamp, A. S. Siddiqui, M. Finlay, and G. J. Barton.** 1998. JPred: a consensus secondary structure prediction server. Bioinformatics **14:**892–893.
15. **Dadgostar, H., and G. Cheng.** 1998. An intact zinc ring finger is required for tumor necrosis factor receptor-associated factor-mediated nuclear factor-κB activation but is dispensable for c-Jun N-terminal kinase signaling. J. Biol. Chem. **273:**24775–24780.
16. **Davidson, S. K., T. A. Koropatnick, R. Kossmehl, L. Sycuro, and M. J. McFall-Ngai.** 2004. NO means 'yes' in the squid-vibrio symbiosis: nitric oxide (NO) during the initial stages of a beneficial association. Cell. Microbiol. **6:**1139–1151.
17. **Devin, A., Y. Lin, S. Yamaoka, Z. Li, M. Karin, and Z. Liu.** 2001. The α and β subunits of IκB kinase (IKK) mediate TRAF2-dependent IKK recruitment to tumor necrosis factor (TNF) receptor 1 in response to TNF. Mol. Cell. Biol. **21:**3986–3994.
18. **Doino, J. A., and M. J. McFall-Ngai.** 1995. A transient exposure to symbiosis-competent bacteria induces light organ morphogenesis in the host squid. Biol. Bull. **189:**347–355.
19. **Dziarski, R.** 2004. Peptidoglycan recognition proteins (PGRPs). Mol. Immunol. **40:**877–886.
20. **Escoubas, J. M., L. Briant, C. Montagnani, S. Hez, C. Devaux, and P. Roch.** 1999. Oyster IKK-like protein shares structural and functional properties with its mammalian homologues. FEBS Lett. **453:**293–298.
21. **Fallon, P. G., R. L. Allen, and T. Rich.** 2001. Primitive Toll signalling: bugs, flies, worms and man. Trends Immunol. **22:**63–66.
22. **Felsenstein, J.** 1989. PHYLIP: phylogeny inference package (version 3.2). Cladistics **5:**164–166.
23. **Foster, J. S., M. A. Apicella, and M. J. McFall-Ngai.** 2000. *Vibrio fischeri* lipopolysaccharide induces developmental apoptosis, but not complete morphogenesis, of the *Euprymna scolopes* symbiotic light organ. Dev. Biol. **226:**242–254.
24. **Foster, J. S., and M. J. McFall-Ngai.** 1998. Induction of apoptosis by cooperative bacteria in the morphogenesis of host epithelial tissues. Dev. Genes Evol. **208:**295–303.
25. **Ghosh, S., M. J. May, and E. B. Kopp.** 1998. NF-κB and Rel proteins: evolutionarily conserved mediators of immune responses. Annu. Rev. Immunol. **16:**225–260.

26. **Gilmore, T. D.** 1990. NF-κB, KBF1, dorsal, and *rel*ated matters. Cell **62:**841–843.
27. **Gilmore, T. D.** 1999. The Rel/NF-κB signal transduction pathway: introduction. Oncogene **18:**6842–6844.
28. **Gueguen, Y., J. P. Cadoret, D. Flament, C. Barreau-Roumiguiere, A. L. Girardot, J. Garnier, A. Hoareau, E. Bachere, and J. M. Escoubas.** 2003. Immune gene discovery by expressed sequence tags generated from hemocytes of the bacteria-challenged oyster, *Crassostrea gigas.* Gene **303:**139–145.
29. **Halanych, K. M., J. D. Bacheller, A. M. Aguinaldo, S. M. Liva, D. M. Hillis, and J. A. Lake.** 1995. Evidence from 18S ribosomal DNA that the lophophorates are protostome animals. Science **267:**1641–1643.
30. **Hoffmann, J. A., F. C. Kafatos, C. A. Janeway, Jr., and R. A. Ezekowitz.** 1999. Phylogenetic perspectives in innate immunity. Science **284:**1313–1318.
31. **Huang, B., M. Eberstadt, E. T. Olejniczak, R. P. Meadows, and S. W. Fesik.** 1996. NMR structure and mutagenesis of the Fas (APO-1/CD95) death domain. Nature **384:**638–641.
32. **Janeway, C. A., Jr.** 1989. Approaching an asymptote? Evolution and revolution in immunology. Cold Spring Harbor Symp. Quant. Biol. **54:**1–13.
33. **Jobin, C., and R. B. Sartor.** 2000. The IκB/NF-κB system: a key determinant of mucosal inflammation and protection. Am. J. Physiol. Cell Physiol. **278:** C451–C462.
34. **Jono, H., T. Shuto, H. Xu, H. Kai, D. J. Lim, J. R. Gum, Jr., Y. S. Kim, S. Yamaoka, X. H. Feng, and J. D. Li.** 2002. Transforming growth factor-α-Smad signaling pathway cooperates with NF-κB to mediate nontypeable *Haemophilus influenzae*-induced *MUC2* mucin transcription. J. Biol. Chem. **277:**45547–45557.
35. **Karin, M., and Y. Ben-Neriah.** 2000. Phosphorylation meets ubiquitination: the control of NF-κB activity. Annu. Rev. Immunol. **18:**621–663.
36. **Karin, M., and A. Lin.** 2002. NF-κB at the crossroads of life and death. Nat. Immunol. **3:**221–227.
37. **Kim, M. S., M. Byun, and B. H. Oh.** 2003. Crystal structure of peptidoglycan recognition protein LB from *Drosophila melanogaster.* Nat. Immunol. **4:**787–793.
38. **Kishino, H., and M. Hasegawa.** 1989. Evaluation of the maximum likelihood estimate of the evolutionary tree topologies from DNA sequence data, and the branching order in hominoidea. J. Mol. Evol. **29:**170–179.
39. **Koropatnick, T. A., J. T. Engle, M. A. Apicella, E. V. Stabb, W. E. Goldman, and M. J. McFall-Ngai.** 2004. Microbial factor-mediated development in a host-bacterial mutualism. Science **306:**1186–1188.
40. **Li, J. D., W. Feng, M. Gallup, J. H. Kim, J. Gum, Y. Kim, and C. Basbaum.** 1998. Activation of NF-κB via a Src-dependent Ras-MAPK-pp90rsk pathway is required for *Pseudomonas aeruginosa*-induced mucin overproduction in epithelial cells. Proc. Natl. Acad. Sci. USA **95:**5718–5723.
41. **Li, Q., and I. M. Verma.** 2002. NF-κB regulation in the immune system. Nat. Rev. Immunol. **2:**725–734.
42. **Liu, C., Z. Xu, D. Gupta, and R. Dziarski.** 2001. Peptidoglycan recognition proteins: a novel family of four human innate immunity pattern recognition molecules. J. Biol. Chem. **276:**34686–34694.
43. **Lomaga, M. A., W. C. Yeh, I. Sarosi, G. S. Duncan, C. Furlonger, A. Ho, S. Morony, C. Capparelli, G. Van, S. Kaufman, A. van der Heiden, A. Itie, A. Wakeham, W. Khoo, T. Sasaki, Z. Cao, J. M. Penninger, C. J. Paige, D. L. Lacey, C. R. Dunstan, W. J. Boyle, D. V. Goeddel, and T. W. Mak.** 1999. TRAF6 deficiency results in osteopetrosis and defective interleukin-1, CD40, and LPS signaling. Genes Dev. **13:**1015–1024.
44. **Marchler-Bauer, A., and S. H. Bryant.** 2004. CD-Search: protein domain annotations on the fly. Nucleic Acids Res. **32:**W327–W331.
45. **Mellroth, P., J. Karlsson, and H. Steiner.** 2003. A scavenger function for a *Drosophila* peptidoglycan recognition protein. J. Biol. Chem. **278:**7059–7064.
46. **Michel, T., J. M. Reichhart, J. A. Hoffmann, and J. Royet.** 2001. *Drosophila* Toll is activated by gram-positive bacteria through a circulating peptidoglycan recognition protein. Nature **414:**756–759.
47. **Miyamoto, S., and I. M. Verma.** 1995. Rel/NF-κB/IκB story. Adv. Cancer Res. **66:**255–292.
48. **Montagnani, C., C. Kappler, J. M. Reichhart, and J. M. Escoubas.** 2004. *Cg*-Rel, the first Rel/NF-κB homolog characterized in a mollusk, the Pacific oyster *Crassostrea gigas.* FEBS Lett. **561:**75–82.
49. **Montgomery, M. K., and M. McFall-Ngai.** 1994. Bacterial symbionts induce host organ morphogenesis during early postembryonic development of the squid *Euprymna scolopes.* Development **120:**1719–1729.
50. **Morin, P. J., A. B. Sparks, V. Korinek, N. Barker, H. Clevers, B. Vogelstein, and K. W. Kinzler.** 1997. Activation of β-catenin-Tcf signaling in colon cancer by mutations in β-catenin or APC. Science **275:**1787–1790.
51. **Nurnberger, T., and F. Brunner.** 2002. Innate immunity in plants and animals: emerging parallels between the recognition of general elicitors and pathogen-associated molecular patterns. Curr. Opin. Plant Biol. **5:**318–324.
52. **Nyholm, S. V., B. Deplancke, H. R. Gaskins, M. A. Apicella, and M. J. McFall-Ngai.** 2002. Roles of *Vibrio fischeri* and nonsymbiotic bacteria in the dynamics of mucus secretion during symbiont colonization of the *Euprymna scolopes* light organ. Appl. Environ. Microbiol. **68:**5113–5122.
53. **Nyholm, S. V., and M. J. McFall-Ngai.** 2004. The winnowing: establishing the squid-vibrio symbiosis. Nat. Rev. Microbiol. **2:**632–642.
54. **Nyholm, S. V., E. V. Stabb, E. G. Ruby, and M. J. McFall-Ngai.** 2000. Establishment of an animal-bacterial association: recruiting symbiotic vibrios from the environment. Proc. Natl. Acad. Sci. USA **97:**10231–10235.
55. **Pikarsky, E., R. M. Porat, I. Stein, R. Abramovitch, S. Amit, S. Kasem, E. Gutkovich-Pyest, S. Urieli-Shoval, E. Galun, and Y. Ben-Neriah.** 2004. NF-κB functions as a tumour promoter in inflammation-associated cancer. Nature **431:**461–466.
56. **Reiser, J. B., L. Teyton, and I. A. Wilson.** 2004. Crystal structure of the *Drosophila* peptidoglycan recognition protein (PGRP)-SA at 1.56 Å resolution. J. Mol. Biol. **340:**909–917.
57. **Rothwarf, D. M., E. Zandi, G. Natoli, and M. Karin.** 1998. IKK-γ is an essential regulatory subunit of the IκB kinase complex. Nature **395:**297–300.
58. **Ruby, E. G., and M. J. McFall-Ngai.** 1999. Oxygen-utilizing reactions and symbiotic colonization of the squid light organ by *Vibrio fischeri.* Trends Microbiol. **7:**414–420.
59. **Ruiz-Trillo, I., J. Paps, M. Loukota, C. Ribera, U. Jondelius, J. Baguna, and M. Riutort.** 2002. A phylogenetic analysis of myosin heavy chain type II sequences corroborates that Acoela and Nemertodermatida are basal bilaterians. Proc. Natl. Acad. Sci. USA **99:**11246–11251.
60. **Salzman, A. L., T. Eaves-Pyles, S. C. Linn, A. G. Denenberg, and C. Szabo.** 1998. Bacterial induction of inducible nitric oxide synthase in cultured human intestinal epithelial cells. Gastroenterology **114:**93–102.
61. **Schultz, J., F. Milpetz, P. Bork, and C. P. Ponting.** 1998. SMART, a simple modular architecture research tool: identification of signaling domains. Proc. Natl. Acad. Sci. USA **95:**5857–5864.
62. **Shaw, P. W.** 1997. Polymorphic microsatellite markers in a cephalopod: the veined squid *Loligo forbesi.* Mol. Ecol. **6:**297–298.
63. **Shekels, L. L., and S. B. Ho.** 2003. Characterization of the mouse Muc3 membrane bound intestinal mucin 5′ coding and promoter regions: regulation by inflammatory cytokines. Biochim. Biophys. Acta **1627:**90–100.
64. **Silverman, N., and T. Maniatis.** 2001. NF-κB signaling pathways in mammalian and insect innate immunity. Genes Dev. **15:**2321–2342.
65. **Small, A. L., and M. J. McFall-Ngai.** 1999. Halide peroxidase in tissues that interact with bacteria in the host squid *Euprymna scolopes.* J. Cell. Biochem. **72:**445–457.
66. **Sokolov, E. P.** 2000. An improved method for DNA isolation from mucopolysaccharide-rich molluscan tissues. J. Moll. Stud. **66:**573–575.
67. **Suzuki, N., S. Suzuki, G. S. Duncan, D. G. Millar, T. Wada, C. Mirtsos, H. Takada, A. Wakeham, A. Itie, S. Li, J. M. Penninger, H. Wesche, P. S. Ohashi, T. W. Mak, and W. C. Yeh.** 2002. Severe impairment of interleukin-1 and Toll-like receptor signalling in mice lacking IRAK-4. Nature **416:**750–756.
68. **Tauszig, S., E. Jouanguy, J. A. Hoffmann, and J. L. Imler.** 2000. Toll-related receptors and the control of antimicrobial peptide expression in *Drosophila*. Proc. Natl. Acad. Sci. USA **97:**10520–10525.
69. **Thompson, J. D., T. J. Gibson, F. Plewniak, F. Jeanmougin, and D. G. Higgins.** 1997. The CLUSTAL_X windows interface: flexible strategies for multiple sequence alignment aided by quality analysis tools. Nucleic Acids Res. **25:**4876–4882.
70. **Tlaskalova-Hogenova, H., R. Stepankova, T. Hudcovic, L. Tuckova, B. Cukrowska, R. Lodinova-Zadnikova, H. Kozakova, P. Rossmann, J. Bartova, D. Sokol, D. P. Funda, D. Borovska, Z. Rehakova, J. Sinkora, J. Hofman, P. Drastich, and A. Kokesova.** 2004. Commensal bacteria (normal microflora), mucosal immunity and chronic inflammatory and autoimmune diseases. Immunol. Lett. **93:**97–108.
71. **Weis, V. M., A. L. Small, and M. J. McFall-Ngai.** 1996. A peroxidase related to the mammalian antimicrobial protein myeloperoxidase in the *Euprymna-Vibrio* mutualism. Proc. Natl. Acad. Sci. USA **93:**13683–13688.
72. **Werner, T., G. Liu, D. Kang, S. Ekengren, H. Steiner, and D. Hultmark.** 2000. A family of peptidoglycan recognition proteins in the fruit fly *Drosophila melanogaster.* Proc. Natl. Acad. Sci. USA **97:**13772–13777.
73. **Yamaoka, S., G. Courtois, C. Bessia, S. T. Whiteside, R. Weil, F. Agou, H. E. Kirk, R. J. Kay, and A. Israel.** 1998. Complementation cloning of NEMO, a component of the IκB kinase complex essential for NF-κB activation. Cell **93:**1231–1240.
74. **Yaron, A., H. Gonen, I. Alkalay, A. Hatzubai, S. Jung, S. Beyth, F. Mercurio, A. M. Manning, A. Ciechanover, and Y. Ben-Neriah.** 1997. Inhibition of NF-κB cellular function via specific targeting of the IκB-ubiquitin ligase. EMBO J. **16:**6486–6494.